Effect of Hydroxylamine on Photosystem II: Reinvestigation of Electron Paramagnetic Resonance Characteristics Reveals Possible S State Intermediates†

Jonathan H. A. Nugent,*,‡ Irine P. Muhiuddin, and Michael C. W. Evans‡

Department of Biology, Darwin Building, University College London, Gower Street, London, WC1E 6BT, U.K.

Received January 21, 2003; Revised Manuscript Received March 20, 2003

ABSTRACT: Previous work in many laboratories has established that hydroxylamine reduces the S_1 state of the water oxidizing complex (WOC) in one-electron steps. Significant levels of what can now be defined as the S_{-1}* state are achieved by specific (concentration and incubation length) hydroxylamine treatments. This state has already been studied by electron paramagnetic resonance spectrometry (EPR), and unusual EPR signals were noted (for example, see Sivaraja, M., and Dismukes, G. C. (1988) *Biochemistry 27*, 3467−3475). We have now reinvestigated these initial experiments and confirmed many of the original observations. We then utilized more recent EPR markers for the S_0 and S_1 states to further explore the S_{-1}* state. The broad radical "split" type EPR signal, produced by 200 K illumination of samples prepared to give a high yield of the S_{-1}* state, is shown to most likely reflect a trapped intermediate state between S_{-1}* and S_0*, since samples where this signal is present can be warmed in the dark to produce S_0*. The threshold for advancement from S_{-1}* to S_0* is near 200 K, as the yield of broad radical decreases and S_0* multiline EPR signal increases with length of 200 K illumination. Advancement of S_0* to S_1 is limited at 200 K, but S_1 can be restored by 273 K illumination. Illumination of these hydroxylamine-treated samples at temperatures below 77 K gives a second broad radical EPR signal. The line shape, decay, and other properties of this new radical signal suggest that it may arise from an interaction in the S_{-2}* or lower S states, which are probably present in low yield in these samples. Illumination below 20 K of S_0* state samples containing methanol, and therefore exhibiting the S_0 multiline signal, gives rise to a third broad radical with distinctive line shape. The characteristics of the three broad radicals are similar to those found from interactions between $Y_Z^\bullet$ and other S states. The evidence is presented that they do represent intermediate states in S state turnover. Further work is now needed to identify these radicals.

A membrane-bound pigment−protein complex called photosystem II (PSII)[1] catalyzes photosynthetic water oxidation in plants, algae, and cyanobacteria. Water oxidation is believed to occur in a complex of four manganese (Mn) atoms, the water oxidizing complex (WOC) accumulating the four oxidizing equivalents required from the PSII reaction center. PSII electron transfer begins with the excitation of the reaction center multi-chlorophyll *a* species termed P680, to P680*, and rapid electron transfer from P680*, via pheophytin, to the bound plastoquinone, Qa, forming $P680^+Qa^{\bullet-}$. Electron transfer then occurs from $Qa^{\bullet-}$ to a second plastoquinone, Qb. Qb accepts two electrons and takes up two protons forming QbH_2, which then dissociates from its site into the membrane. A non-heme iron usually present as Fe^{2+}, which can be oxidized under some conditions, is situated between Qa and Qb. $P680^+$ extracts an electron from the WOC via a tyrosine electron carrier termed Y_Z, forming $Y_Z^\bullet$, the neutral tyrosine radical (*1*−*3*). A tyrosine on polypeptide D2 (PsbD) termed Y_D can also be photooxidized by PSII but is not on the main electron-transfer pathway (see reviews *1*−*3*). Cytochrome b559 (Cyt b559), a chlorophyll termed Chl Z, and a carotenoid can also be secondary electron donors to oxidized P680 under some conditions (*1*−*3*). The reduction kinetics of $P680^+$ by Y_Z, and subsequently of $Y_Z^\bullet$ by the WOC, is dependent on the S state. Although a large fraction of $P680^+$ is reduced by Y_Z in nanoseconds, slower phases also occur (*4*−*6*). Y_Z has been proposed to be involved in the water oxidation process itself, as a hydrogen atom abstractor or in promoting proton-coupled electron transfer from the WOC (*1*−*3*, *7*−*14*).

During water oxidation, the WOC passes through redox states termed S states. Electrons are removed on each step from S_0 to S_4, and oxygen is evolved at the transient S_4 state, formed during the S_3−S_0 step (*1*−*3*, *15*, *16*). The oxidation of the WOC must be an almost electroneutral process in order for it to occur within the limitations imposed by reaction center chemistry and energetics. Proton release to the lumen during the S state cycle provides the necessary charge balance to electron transfer.

† Financial assistance from the U.K. Biotechnology and Biological Sciences Research Council and the Leverhulme Trust is acknowledged.

* To whom correspondence should be addressed. Fax: +44 (0)20 7679 7096; E-mail: j.nugent@ucl.ac.uk. Phone: +44 (0)20 7679 2681.

‡ J.H.A.N. and M.C.W.E. are members of the Bloomsbury Centre for Structural Biology at UCL and Birkbeck College.

[1] Abbreviations: EDTA, ethylenediaminetetraacetic acid; EPR, electron paramagnetic resonance spectrometry; DCMU, 3-(3,4-dichlorophenyl)-1,1-dimethylurea; DCBQ, 2,5 dichlorobenzoquinone; WOC, water oxidizing complex; PSII, photosystem II; MES, 2-(*N*-morpholino)-ethanesulfonic acid; Chl, chlorophyll; Qa, the first PSII plastoquinone electron acceptor; Qb, the second PSII plastoquinone electron acceptor; Y_Z, tyrosine D1 161 ($Y_Z^\bullet$ when oxidized); Y_D, tyrosine D2 161 ($Y_D^\bullet$ when oxidized); Cyt b559, cytochrome b559; P680, PSII primary electron donor; NIR, near-infrared light.

10.1021/bi034116u CCC: $25.00
Published on Web 04/16/2003

The S_2 and S_3 states are unstable with short half-lives at room temperature. Both decay back to S_1 (*1*−*3*). Therefore, after a few minutes in the dark, about 75% of PSII is in S_1 and 25% in S_0. During further dark adaptation, the S_0 state is slowly oxidized to S_1 by $Y_D^{\bullet}$ (*1*−*3*). EPR signals that characterize the S_0 (*17*−*19*), S_1 (*20*−*23*), S_2 (*24*−*27*), and S_3 states (*28*−*30*) have now been observed. The addition of methanol is required in order to observe the S_0 (spin $S = {}^1/_2$) multiline signal (*17*−*19*). S_2 EPR signals include an $S = {}^1/_2$ multiline signal centered near $g = 2$ (*24*, *25*) and an $S \geq {}^3/_2$ signal at $g = 4.1$ (*26*, *27*). The latter is removed by alcohols such as methanol, which also slightly modifies the hyperfine splitting of the $S = {}^1/_2$ multiline signal. The S_1 ($g = 4.8$ or 12) and S_3 states are characterized by weak integer spin signals observed by parallel mode EPR (*20*−*23*, *29*, *30*).

Y_Z is near the Mn cluster (*31*), and when both are paramagnetic (i.e., $Y_Z^{\bullet}$ plus a paramagnetic Mn cluster), they can interact to give complex, broad EPR "split" signals at cryogenic temperatures. This type of signal was initially reported in samples where oxygen evolution was inhibited at the S_2−S_3 step (*32*−*34*), and these are now assigned to a $S_2Y_Z^{\bullet}$ state (*35*−*37*). We reported experiments suggesting that an interaction between an organic radical and the Mn cluster (probably $S_2Y_Z^{\bullet}$) could be observed in uninhibited PSII and that this was related to formation of S_3 (*28*). This work was extended by Petrouleas and co-workers (*30*), and recently we have characterized the relationship between the EPR signals arising from the S_3 state and intermediate states (including $S_2Y_Z^{\bullet}$) that can form it (*38*, *39*).

We have also recently shown that the S_1−S_2 step can occur at very low temperatures, a result that has important implications for the nature of Y_Z. We characterized a signal initially attributed to the interaction between S_1 and $Y_Z^{\bullet}$ as an intermediate state between the S_1 and S_2 states (*40*).

In this paper, we investigate previous reports of unusual EPR signals in hydroxylamine-treated PSII. To indicate that the electronic configuration of hydroxylamine-treated samples may be different to native S states, although equivalent in reduction level, the notation S_0*, S_{-1}*, etc. will be used as in an earlier paper (*41*). Hydroxylamine has been shown in many studies to reduce the S_1 state to lower S states (*41*−*52* and references therein) in one-electron steps. Hydroxylamine acts at the type 2 (Cl^-) amine-binding site of the WOC (*51*, *52*). The rate of reduction of S_0* to S_{-1}* is approximately twice as fast as S_1 to S_0* (*48*). Although a mixture of S states is produced by hydroxylamine treatment, conditions can be devised where S_{-1}* is the major product as characterized by a two-flash delay in either oxygen evolution or S_2 multiline formation (*42*, *43*, *45*−*47*).

The EPR characteristics of hydroxylamine-treated samples were studied in detail in the late 1980s (*45*−*47*). These studies can be briefly summarized as showing that at low hydroxylamine concentrations, a short incubation gave a reversible reduction to mostly S_{-1}*, whereas at high concentrations further reduction of Mn and irreversible changes including release of Mn^{2+} occurred. At that time, only a two-turnover delay in formation of the S_2 multiline EPR signal could be used to monitor the treatments because no S_0 or S_1 markers were available. One unusual new signal was observed (*45*−*47*): a broad radical signal formed by 200 K illumination after treatment with low hydroxylamine concentrations (5−10 molecules of hydroxylamine/PSII for short incubation times). This was attributed to an unspecified electron acceptor component (*45*−*47*). No nitroxide radicals were produced by this hydroxylamine treatment (*45*). More recently hydroxylamine treatment was used to produce the first EPR signal from the S_0 state (*17*), the S_0* multiline signal line shape later being shown to be virtually identical to that of the S_0 signal produced by flash turnover of untreated PSII (*18*, *19*).

In this study, we use the known effects of hydroxylamine at low concentration to reversibly reduce the dark-adapted S_1 state. We then use S_0, S_1, and S_2 EPR markers to investigate the effect of illumination of the reduced sample at various temperatures. In particular, we examine the characteristics of the broad radical signal and compare it to the $S_2Y_Z^{\bullet}$ broad radical signals.

MATERIALS AND METHODS

Sample Preparation. PSII membranes were prepared from 10 to 14 day old pea seedlings using Triton X-100, using the modifications of Ford and Evans (*53*). Reagents used were all analytical grade. Chlorophyll concentration (Chl) was measured by the method of Porra (*54*). Control rates of oxygen evolution for PSII membranes were 500−1100 (μmol of O_2)·(mg of Chl)$^{-1}$·h^{-1} using ferricyanide and dimethylbenzoquinone as electron acceptors and measured in an oxygen electrode at 298 K. The membranes were stored at 77 K in 20 mM 2-(*N*-morpholino)ethanesulfonic acid (MES), 15 mM NaCl, 5 mM $MgCl_2$, 0.4 M sucrose, pH 6.3 (buffer A). Before preparation of EPR samples, the PSII membranes were (except where stated) washed in buffer A containing 2 mM ethylenediaminetetraacetic acid (EDTA) to remove adventitiously bound Mn^{2+}, followed by centrifugation and resuspension in buffer A. Removal of Mn from the WOC was achieved using Tris washing at high pH as given in ref *28* or by high concentration of hydroxylamine (2 mM for 30 min) followed by centrifugation and resuspension in buffer A.

For EPR, 0.3−0.4 mL samples (approximately 6−10 mg Chl/mL, 25−40 μM PSII) were placed in calibrated ~3 mm quartz EPR tubes. Identical sets of samples in calibrated EPR tubes were made for each experiment, using the same preparation and chlorophyll concentration. They were given a brief (30 s) illumination at 277 K to turn over the PSII reaction center and to restore the $Y_D^{\bullet}$ lost on storage. Additional procedures were carried out in the dark or under a dim green light.

Samples were dark-adapted for 2 h at 273 K and then treated as described in the text and figure legends. Methanol was used at 1.5% final concentration. Treated or untreated samples were dark-adapted following additions before being frozen to 77 K in the dark (total dark adaptation of ~3 h). In untreated samples, this produced samples initially in the S_1 Qa state, as indicated by the absence of the S_2 EPR markers, the multiline signal or the $g = 4.1$ signal, and $Qa^{\bullet -}$. Absence of photosystem I was confirmed by the lack of signals from oxidized P700 or reduced iron−sulfur centers A or B following illumination at <30 K. The signals present in control samples (Cyt b559, etc.,) were directly compared during experiments that involved EPR data collection on different days. This confirmed the reproducibility of spectra

so that no normalization was required or performed. Precautions to exclude EPR signals from oxygen were as previously described (*28*). Careful wiping of the tubes prior to insertion into the cryostat also helps to prevent frozen oxygen from condensing on the tube or sample surface and thereby distorting spectra.

Hydroxylamine Treatment. EDTA-washed PSII membranes were loaded into EPR tubes and dark-adapted for 2 h on ice. Hydroxylamine was then added to give a particular ratio of hydroxylamine/PSII (a range of 5−10 hydroxylamine/PSII was tested). This treatment was chosen from the experiments in refs *45*−*47* and the equilibrium titrations performed in ref *46*. After a specific incubation time, of either 15 or 30 min on ice, the sample was frozen to 77 K or 1 mM 2,5-dichlorobenzoquinone (DCBQ) in dimethyl sulfoxide (DMSO, final concentration of 1%) was added to stop the reaction by oxidation of excess hydroxylamine and also to ensure oxidation of PSII quinone electron acceptors (*45*). The sample was frozen 15 min after addition of DCBQ.

EPR. Samples were illuminated at a variety of temperatures. Illumination in the EPR cavity at <30 K involved a 150 W light source and fiber-optic light guide, while other illuminations involved a 1000 W light source, protecting the sample from heating where necessary by a 5 cm water filter. Where necessary, near-infrared (NIR) light was excluded from illuminated samples by using an Ealing Electrooptics long wavelength cutoff filter (50% transmission at 661.6 nm, ∼0 above 700 nm). Samples for 77 K dark adaptation or illumination were placed in liquid nitrogen in a silvered Dewar, while samples for 200 K illumination were placed in an ethanol/dry ice bath in an unsilvered clear glass Dewar. The temperature of the bath was measured by thermometer. Temperatures within the EPR cryostat were measured with a calibrated thermocouple placed beneath the sample. Once the cryostat temperature reached equilibrium, the temperature could be maintained within ±0.1 K for several hours if required. At <20 K, any slight changes caused by heating during illumination were reversed by the helium flow in less than 1 min. Heating effects due to illumination have been studied and minimized as in ref *40*. In some cases spectra from illuminated samples were recorded a short time (usually 1 min) after illumination to check for heat-induced effects. Heat-induced effects can easily be detected and roughly quantified as a sudden change in signal size when turning the light on or off.

Samples were examined by EPR at cryogenic temperatures using a JEOL RE1X spectrometer fitted with an Oxford Instruments cryostat. EPR conditions are given in the figure legends. Spectra were recorded and manipulated using a Dell microcomputer running Asyst software, and spectra were plotted using Microsoft Excel. No filtering, smoothing, fitting, or background subtractions were used. Difference spectra were obtained only by subtraction of spectra from the same sample. The vertical scale in figures showing first derivative EPR spectra is arbitrary, with spectra measured at the same instrument gain unless otherwise stated in the figure legend. The field scale corresponds to g values as follows: $g = 6$ at 107.6 mT; $g = 3$ at 215.2 mT; $g = 2$ at 322.8 mT. A standard S_0* sample was prepared using hydroxylamine as in ref *17*. The amplitude of split $g = 2$ signals was measured as the peak to trough height from the light on minus the dark difference spectrum.

RESULTS

To investigate the hydroxylamine-treated samples, we used three EPR signals as markers for the S_0, S_1, and S_2 states.

(a) In dark-adapted S_1 state samples, <20 K illumination produces a broad radical signal that we have shown is a marker for an intermediate state between S_1 and S_2 (*40*). This will be termed the S1 broad radical.

(b) A 200 K illumination of an S_1 state sample produces almost complete conversion to the S_2 state with formation of the S_2 multiline near $g = 2$ and $g = 4.1$ signals (*24*−*27*). The S_2 multiline is observed in the absence of methanol.

(c) In hydroxylamine-treated samples, the S_0* state multiline signal can be monitored. The S_0* multiline is only observed following the addition of methanol (*17*−*19*). The S_0* multiline has a distinctive EPR line shape, but also the effect of methanol clearly distinguishes the S_0 signal and S_2 state multiline signals (*55*).

In our initial experiments, we confirmed the EPR investigations by previous authors (*45*−*47*) in that treatment at 5−10 molecules of hydroxylamine/PSII for short periods (15−30 min) causes a loss of ability to generate the S_2 multiline by 200 K illumination. A treatment of ∼6 hydroxylamine/PSII was then selected. Only a very small (<5%) release of Mn^{2+} was observed by these low concentrations of hydroxylamine (in samples lacking EDTA), in agreement with the results in refs *45*−*47*. The ability to produce the S1 broad radical was lost, and only very small amounts of S_0* multiline signal were detected (see below). A broad radical similar to that found in refs *45*−*47* was induced by 200 K illumination (see below). The EPR microwave power saturation properties of this signal suggest involvement of a rapidly relaxing paramagnetic transition metal center or complex (see *45*−*47*). The observations confirm that the S_1 state has been reduced and that the conditions used were similar to those in refs *45*−*47* where S_{-1}* was the major state produced.

Broad Radical Signals. Figure 1A−C show the different broad "split" radical signals obtained from (∼6 hydroxylamine/PSII) treated PSII after 2 min of illumination at 8 K (Figure 1A) and 200 K (Figure 1B), of DCBQ-containing samples, and 77 K illumination (4 min) of a sample without DCBQ (Figure 1C). It can be seen that a rather narrow line shape is obtained by <20 K illumination (8 K, Figure 1A) while a much broader line shape is present following 200 K illumination (Figure 1B). Investigation of several sets of samples indicates that 77 K illumination produces a mixture of both forms, mainly the broader form but with the line shape varying slightly between different hydroxylamine-treated PSII preparations. Use of an NIR filter during the 77 K illumination does not prevent observation of the broad radical (not shown). The EPR microwave power required to observe the signals suggests the involvement of a rapidly relaxing paramagnetic transition metal center or complex. Figure 1C also shows that the absence of DCBQ increases the yield of photo-oxidized Cyt b559 (g_y peak visible at ∼300 mT in Figure 1C). DCBQ decreases the competition from Cyt b559 electron donation during illumination at cryogenic temperatures as the DCBQ treatment increases the level of oxidized Cyt b559 in the dark-adapted sample following preparation (*40*).

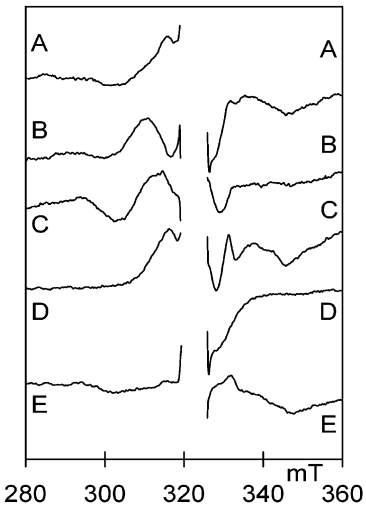

FIGURE 1: EPR spectra showing the formation of the broad radicals in hydroxylamine-treated PSII at 8 K. Chlorophyll concentration was 9 mg/mL (~36 μM PSII), and the hydroxylamine/PSII ratio was ~6. Samples were DCBQ-treated except for sample for Figure 1C. (A) Illuminated at 8 K (2 min) minus dark difference spectrum. (B) Illuminated at 200 K (2 min) minus dark difference spectrum. (C) Illuminated at 77 K (4 min) minus dark difference spectrum. (D) Reilluminated at 8 K minus illuminated at 8 K then dark at 8 K for 20 min difference spectrum. (E) Tris-washed hydroxylamine-treated PSII sample (8 mg Chl /ml, hydroxylamine/PSII ratio of ~6). Illuminated at 200 K (2 min) minus dark difference spectrum. EPR conditions are the followng: temperature 8 K, modulation amplitude 1.6 mT, microwave power 10 mW. The large $g = 2$ organic radical peak has been omitted.

The "split" signal produced by illumination at 8 K as in Figure 1A decayed in the dark in a few minutes at 8 K following illumination (see Figure 3). Re illumination of the sample at 8 K restores the signal, and the light-induced difference spectrum (Figure 1D) enables the line shape to be seen more clearly because other changes seen only on the first illumination are excluded. This time scale of signal decay (a few minutes at ~10 K) is similar to that observed for the "split" radicals observed previously and attributed to S_1/S_2 (*40*) and S_2/S_3 (*17*, *38*, *39*) intermediate states.

The Mn complex of the WOC can be removed either by incubation with high concentrations of hydroxylamine or by a process termed Tris washing (see Materials and Methods). In ref *45*, it was stated, but not shown, that the broad radical formed by 200 K illumination could be observed in hydroxylamine-treated Tris-washed samples, whereas in contrast, refs *46* and *47* show that the ability to produce the broad radical was clearly lost at high concentrations of hydroxylamine where Mn^{2+} was released. Our results agree with the latter results (*46*, *47*). Figure 1E shows that a hydroxylamine-treated (~6 hydroxylamine/PSII) Tris-washed PSII sample does not show any broad radicals on illumination at 200 K. Only the Qa iron semiquinone signal can be seen, with a very small yield of Cyt b559. The evidence suggests that an intact WOC is required in order to observe the broad radical signals.

Figure 2A shows the S1 broad radical EPR signal obtained by illumination of PSII in the S_1 state as described in ref *40*. This radical was provisionally assigned to an intermediate state between S_1 and S_2, perhaps $S_1Y_Z^{\bullet}$ (*40*). Part of the Qa iron semiquinone signal is seen at high field (e.g., the trough at ~345 mT). Figure 2B shows that the same radical can be obtained following illumination of hydroxylamine-treated

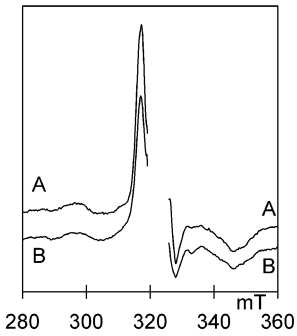

FIGURE 2: EPR spectra showing the formation of the "S1 split signal" at 8 K. The chlorophyll concentration and hydroxylamine/PSII ratio are as indicated for Figure 1. Spectra are the illuminated at 8 K minus dark difference spectra. (A) PSII containing DCBQ (1mM). (B) Hydroxylamine-treated PSII containing DCBQ (1 mM), illuminated at 277 K followed by 60 min dark adaptation. Other EPR conditions are as indicated for Figure 1.

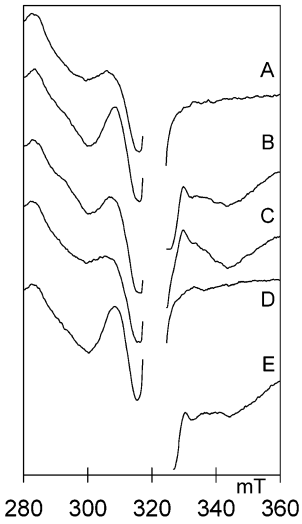

FIGURE 3: EPR spectra at 6 K showing the decay properties of the broad radical formed in hydroxylamine-treated PSII. The chlorophyll concentration and hydroxylamine/PSII ratio are as indicated for Figure 1. Samples were DCBQ-treated: (A) dark; (B) illuminated at 77 K for 4 min; (C) sample in (B) following 15 min at 6 K; (D) sample in (C) following thawing to 288 K and refreezing within 1 min ("annealing"; see Materials and Methods); (E) sample in (D) following reillumination at 77 K for 4 min. Other EPR conditions are as indicated for Figure 1.

PSII (~6 molecules/PSII) at 277 K followed by 60 min of dark adaptation. This confirms the earlier work (*45*−*47*) showing that the S state reduction caused by this level of hydroxylamine treatment is largely reversible (~80% in this sample).

Figure 3 shows that the "split" signal (~305 mT) produced by 77 K illumination (Figure 3B) of a dark-adapted hydroxylamine-treated PSII sample (Figure 3A) decays substantially in 15 min at 6 K in the dark (Figure 3C), while the underlying signal from the $Qa^{\bullet-}$ iron semiquinone decreases slightly. If a sample identical to that shown in Figure 3B is rapidly thawed at 288 K and refrozen (within 1 min), the "split" signal is completely removed (Figure 3D) but can then be restored by further illumination at 77 K, in this case with a slightly increased yield (Figure 3E).

In contrast, the broader radical state produced by 200 K illumination (Figure 1B) is much more stable, only decaying very slowly on storage at 77 K in the dark (not shown). In

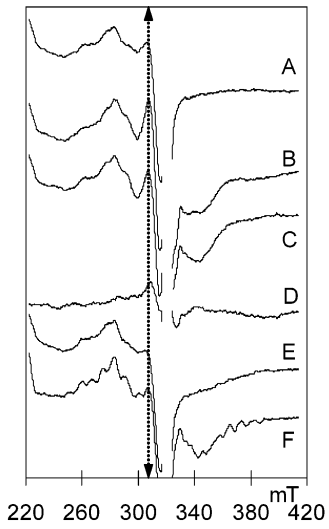

FIGURE 4: EPR spectra at 6 K showing the properties of the broad radical formed in hydroxylamine-treated PSII. Chlorophyll concentration was 9 mg/mL (~36 μM PSII), and the hydroxylamine/PSII ratio was ~6. Samples were DCBQ-treated: (A) dark; (B) illuminated at 200 K for 3 min; (C) sample in (B) illuminated at 200 K for an additional 3 min; (D) difference spectrum of (B) minus (C); (E) identical sample given three cycles of 200 K illumination (3 min) followed by thawing to 288 K and refreezing within 1 min ("annealing" see Materials and Methods); (F) sample in (E) following an additional 3 min of illumination at 200 K. The dotted line indicates the approximate field position for the major peak of the split signal below $g = 2$. Other EPR conditions are as indicated for Figure 1.

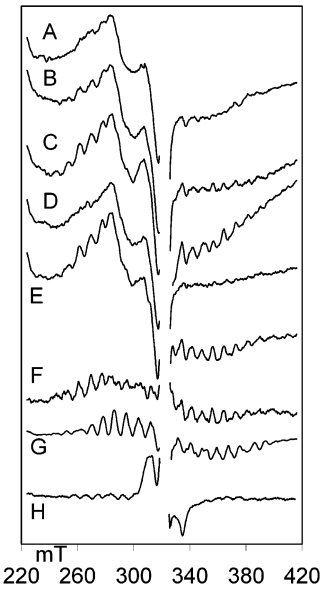

FIGURE 5: EPR spectra at 8 K showing the properties of the multiline signals formed in hydroxylamine-treated PSII. Chlorophyll concentration was 9 mg/mL (~36 μM PSII), and the hydroxylamine/PSII ratio was ~6. Samples were DCBQ-treated: (A) dark sample containing 1.5% methanol; (B) sample in (A) following two cycles of illumination at 77 K for 5 min and annealing (see Figure 4); (C) sample in (A) following illumination at 200 K for 3 min; (D) dark sample following illumination at 200 K for 3 min and annealing; (E) sample in (D) following thawing and addition of 1.5% methanol in the dark; (F) difference spectrum of (E) minus (D) showing the effect of methanol addition causing the S_0* multiline spectrum to be seen; (G) 200 K illuminated minus dark spectrum of an untreated PSII sample in S_1 showing the S_2 multiline spectrum; (H) sample as in (E) (S_0*) illuminated at 8 K. This spectrum is the average of those from three samples. Other EPR conditions are as indicated for Figure 1.

additional experiments examining the illumination of hydroxylamine-treated samples at 200 K, it was also observed that the yield of the broad radical decreased as illumination times were increased. Figure 4A shows the EPR spectrum of hydroxylamine-treated (~6/PSII) PSII, the main peaks being those from Cyt b559 ($g_z \approx 220$ mT and $g_y \approx 290$ mT). Figure 4B shows the broad radical produced by 200 K illumination at 3 min of illumination and the decreased yield observed after an additional 3 min of illumination at 200 K (Figure 4C). The Cyt b559 peaks are unchanged. The dotted line indicates the approximate field position for the major peak of the split signal below $g = 2$. The loss of broad radical is shown in the Figure 4B minus Figure 4C difference spectrum (Figure 4D). Further experiments showed that with our illumination protocol the maximum yield of broad radical was reached after ~1 min of illumination at 200 K and that 200 K illumination for 18 min reduced the yield to ~50%. This indicates that a slow forward process from the broad radical state occurs at 200 K.

Cycles of 3 min of illumination at 200 K, followed by thawing in the dark at 285 K and rapid refreezing within 1 min ("annealing"), were performed to see if S state advancement would occur and if an S_2 multiline signal could be formed. The S_1-S_2 step occurs readily at 200 K (*1*−*3*), and the annealing step allows reoxidation of $Qa^{\bullet-}$. This experiment therefore investigates the threshold temperatures for S_{-1}* to S_0* and S_0* to S_1 turnovers in hydroxylamine-treated PSII. Following two cycles of 200 K illumination and thawing, the third 200 K illumination and thawing cycle produced almost no S_2 multiline EPR signal (Figure 4E; see also refs *45*−*47*). This demonstrates that there is some inhibition of S state turnover between S_{-1}* and S_1 at 200 K. Following three cycles of 200 K illumination and thawing, the fourth 200 K illumination produced only a small yield of S_2 multiline. Figure 4F shows the EPR spectrum after the fourth illumination of these cycles. The ability to form the broad radical by 200 K illumination has been lost, and a small yield of S_2 multiline (<20% of a control untreated S_1 state sample illuminated at 200 K) has been formed. This latter result agrees with similar experiments in refs *45*−*47*.

These results indicate that the S_{-1}*−S_0* transition may occur following illumination at 200 K and annealing (i.e., loss of broad radical) and that the S_0*−S_1 transition is restricted at 200 K (inability to form S_2; see also refs *45*−*47*). The restriction of the S_0-S_1 transition at 200 K was also shown in flash turnover experiments on untreated PSII (*56*). This restriction can be overcome by illumination at 277 K as shown by the restoration of the S1 broad radical in Figure 1.

Mn Multiline EPR Signals. As already shown, cycles of 200 K illumination lead to loss of ability to generate the broad radical, with only a small yield of S_2 multiline signal present even after several turnovers at 200 K. This shows that most centers are trapped below S_1 following 200 K annealing cycles. Therefore, we looked for the S_0 multiline signal in hydroxylamine-treated samples.

Figure 5A shows the EPR spectrum of hydroxylamine-treated (~6/PSII) PSII treated with 1.5% methanol. The addition of methanol should reveal any S_0 state present as an S_0* multiline signal (*17*). Only a very small signal is observed on close inspection of the spectra, suggesting that

S_0 is not present in significant yield after this hydroxylamine treatment. Figure 5B shows the effect of two cycles of 77 K illumination (5 min) and annealing; a small yield of S_0* multiline (see below) is now detected. This indicates that 77 K illumination allows some formation of an intermediate state that can proceed to S_0* on warming. Figure 5C shows the spectrum of a sample identical to that in Figure 5A following only 3 min of 200 K illumination. This produces an S_0* multiline, and the broad radical signal is also present (in reduced yield to samples without methanol, Figure 4). Because formation of S_0* is observed, the forward reaction from S_{-1}* to S_0* occurs in methanol-treated samples at 200 K.

S_0 and S_2 line shapes can be difficult to distinguish. To confirm that S_0 was being formed, hydroxylamine-treated PSII was illuminated at 200 K and annealed (Figure 5D). The sample was then thawed again in the dark, 1.5% methanol was added, and the sample was refrozen. This produces a Mn multiline signal (Figure 5E). The requirement for methanol in order to observe the multiline signal confirms it as S_0*. Figure 5F shows the difference spectrum caused by the methanol addition. A good yield of the S_0* state is obtained. From several experiments, the yield of S_0* obtained was equivalent to, or slightly higher than, that obtained in ref *17* by turnover of hydroxylamine and 3-(3, 4-dichlorophenyl)-1,1-dimethylurea (DCMU) treated samples from S_{-1}* to S_0* by illumination above 273 K. The DCMU was added to restrict the PSII to a single turnover (*17*).

For comparison of line shapes, the S_2 multiline EPR spectrum is shown in Figure 5G. The S_0* spectrum (which is indistinguishable from the S_0 multiline obtained by flash turnover) is weaker in intensity but broader in line shape with more lines than the S_2 multiline (*17*−*19*). Further illumination of the sample in Figure 5E at <20 K produces a new broad radical signal shown in Figure 5H. Small changes in the multiline signal also occur as reflected in the difference spectrum indicating involvement of the Mn cluster. The broad radical signal is only observed in samples treated as here or in ref *17* to produce the S_0* state and that also have methanol added to reveal the S_0* multiline signal. This shows that the addition of methanol to the S_0* state creates the conditions to observe this signal. Without methanol, only the narrower signal as in Figure 1A is observed.

DISCUSSION

In this work we have built upon the considerable amount of existing data concerning the effects of hydroxylamine treatment on PSII (*41*−*52* and references therein). We show clearly that treatment with low concentrations of hydroxylamine produces a sample where the S_{-1}* state is a major product. The S_{-1}* state is confirmed as having no obvious spectrum in perpendicular mode EPR (*45*−*47*). We show that the S_0* state can be obtained by illumination of the hydroxylamine-treated sample, with a threshold temperature around 200 K. Illumination up to 200 K produces an intermediate state that will form S_0* on warming in the dark. This illumination also produces a broad "split" radical that has characteristics expected of the intermediate state between S_{-1}* and S_0*. The broad radical is associated with PSII retaining the WOC as in refs *46* and *47*.

The loss of the broad radical observed in ref *46* following DCMU treatment was probably due to the combined effect of methanol (the solvent for additions in ref *46*) lowering the yield of signal at 200 K (see results above) and to DCMU changing the properties of PSII slightly. This has been shown to lower the yield of other "split" radicals (e.g., in refs *35* and *40*).

The broad radical obtained by illumination at 200 K in S_{-1}* was previously observed and assigned to the formation of an unspecified PSII electron acceptor component (*45*−*47*). This was probably due to the fact that the spectra of the broad radical and the iron semiquinone $Q_A^{\bullet-}$ overlap and cancel/distort the spectrum of the latter. No electron donor was identified as providing the electron in these earlier studies (*45*−*47*). The involvement of Y_Z was not considered because the work preceded the discovery of "split" type broad radicals and the consensus view at that time was that Y_Z did not undergo redox reactions below ∼250 K. Since these earlier studies, a large literature has formed on similar broad or "split" radicals, some of which have been identified as being from an interaction between S_2 and $Y_Z^{\bullet}$. Others have been identified to be in association with intermediate states between S states, with indications that they may also involve $Y_Z^{\bullet}$.

Y_Z has been shown to operate at cryogenic temperatures in some other S states (*28*, *39*, *40*). We now also know much more about the behavior of the electron acceptors of PSII, and no other broad radicals with the overall characteristics (line shape, relaxation properties, formation and decay properties, etc.) have been associated with the electron acceptors of PSII (*28*, *40*). Therefore, the characteristics of the broad radical formed from S_{-1}* now point to the involvement of the Mn cluster and an organic radical. The radical cannot be identified in these present studies, but as argued previously, it is most likely $Y_Z^{\bullet}$ because this is the only established component between P680 and the WOC. The S_{-1}* state would then be a paramagnetic even spin state ($S = 1$, $S = 2$, etc.) and may be observable in parallel mode EPR experiments. The characteristics of the broad radical observed in S_{-1}* are compatible with the observed relatively weak magnetic coupling of $Y_Z^{\bullet}$ with the spin of Mn in both inhibited and untreated preparations, as well as with the crystallographic data (*31*), suggesting a ∼7 Å closest distance between tyrosine and the Mn.

Two new "split" radicals were also detected in this study: the rather narrow radical observed following illumination of S_{-1}* samples in the EPR cavity (Figure 1) and the radical shown in Figure 5 following illumination of methanol-treated S_0* samples in the EPR cavity. The latter signal was only observed following the addition of methanol to produce the S_0* multiline state. It is therefore logical to suggest that this signal represents an intermediate between S_0* and S_1. The radical formed following illumination of S_{-1}* samples in the EPR cavity is more difficult to assign. It is formed in low yield, and because the samples possibly contain several S states, it cannot be linked to any particular one without establishing the link to particular Mn signals as found for other "split" radicals.

Model of Y_Z Turnover. There is general agreement that Y_Z in the oxidized state is neutral (i.e., effectively deprotonated). The nature of the protonation state when the tyrosine is reduced is less obvious. It is often assumed that a protonated neutral tyrosine is present, and this is in line with models suggesting a proton (or H atom) abstraction role of

Scheme 1

A.

$$\mathbf{H^+...Mn^n \ .....(H^+).....Y_Z....H^+.....B^-}$$

$$\mathbf{\leftarrow H^+ \quad Mn^n \ ...(H^+).....Y_Z^{\bullet}.....H^+..B^-}$$

$$\mathbf{Mn^{n+1}.....(H^+).....Y_Z....H^+.....B^-}$$

$(\mathbf{H^+})$ = hydrogen bonding network including water

B.

$$\mathbf{S_{-1}^* \xrightarrow[<200\ K]{} S_{-1}^* Y_Z^{\bullet} \xrightarrow[>200\ K]{} S_0^* \rightarrow S_0^* Y_Z^{\bullet} \xrightarrow[>200\ K]{} S_1}$$

this tyrosine (*1*−*3*, *7*−*14*). Other groups favor a deprotonated tyrosine (*1*−*3*, *7*−*14*).

Various models suggest two extremes for the mechanism of proton release; electrostatic deprotonation and translocation into the lumen versus translocation via a hydrogen-bonded network from Y_Z. We recently proposed a more flexible model between these extremes (*39*). We assume that water associated with the Mn cluster is in hydrogen-bonding contact with Y_Z. We proposed that an array comprising this water and adjacent water (or OH or O) ligands to Mn, followed by a sequence of proton acceptors, acts as an efficient proton translocation pathway under normal circumstances. The model uses electrostatic effects to drive the process in an energetically finely tuned system. It is not surprising that even slight modifications of the WOC cause significant changes to the system. Oxidation of Y_Z therefore repels the hydrogen-bonding proton toward the cluster and initiates proton translocation via the cluster. This role of Y_Z in the water-splitting process is described as an electron abstractor, proton repeller (see Scheme 1A and ref *39*).

The electron-transfer reactions to oxidized P680 can be thought of in two parts. (1) In the first part, an electron is transferred from Y_Z to P680, creating $Y_Z^{\bullet}$. This displaces the phenolic proton toward the base (probably D1 His 190), and the increase in positive charge causes proton loss from the Mn complex or water. This reduces the redox potential of the Mn complex. Tunneling of H-bonded protons is thought to occur even at cryogenic temperatures (*57*).

(2) In the second part, an electron is transferred from the Mn complex to $Y_Z^{\bullet}$. The strength of the hydrogen bonding to Y_Z will depend on the S state, the extent of deprotonation of the Mn cluster, and environmental factors (e.g., pH). Y_Z will be a good low-temperature donor in those S states and in the fraction of centers where the Mn cluster is deficient of protons. Y_Z is a good low-temperature electron donor in S_1 (*40*). This may relate to the observed <1 proton release during the S1−S2 transition (*1*−*3*). Also, $Y_Z^{\bullet}$ appears to be readily formed by the low-temperature illumination of the proton-deficient S2′ state (*28*, *30*, *38*, *39*). In this work, the threshold to complete the $S_{-1}-S_0$ transition is about 200 K whereas the S_0-S_1 transition only occurs at higher temperatures (*56*) (Scheme 1B).

REFERENCES

1. Diner, B. A., and Babcock, G. T. (1996) in *Oxygenic Photosynthesis: The Light Reactions* (Ort, D. R., and Yocum, C. F., Eds.), pp 213−247, Kluwer Academic Publishers, Dordrecht, The Netherlands.
2. Britt, R. D. (1996) in *Oxygenic Photosynthesis: The Light Reactions* (Ort, D. R., and Yocum, C. F., Eds.), pp 137−164, Kluwer Academic Publishers, Dordrecht, The Netherlands.
3. Nugent, J. H. A. (1996) *Eur. J. Biochem. 237*, 519−531.
4. Lavergne, J., and Junge, W. (1993) *Photosynth. Res. 38*, 279−296.
5. Schilstra, M. J., Rappaport, F., Nugent, J. H. A., Barnett, C. J., and Klug, D. R. (1998) *Biochemistry 37*, 3974−3981.
6. Christen, G., Seeliger, A., and Renger, G. (1999) *Biochemistry 38*, 6082−6092.
7. Nugent, J. H. A., Rich, A. M., and Evans, M. C. W. (2001) *Biochim. Biophys. Acta 1503*, 138−146.
8. Hoganson, C. W., and Babcock, G. T. (1999) in *Biological Processes. Metal Ions in Biological Systems* (Sigel, A., and Sigel, H., Eds.), Vol. 37, pp 613−656, Marcel Dekker, New York.
9. Hoganson, C. W., Lydakis-Simantiris, N., Tang, X.-S., Tommos, C., Warncke, K., Babcock, G. T., Diner, B. A., McCracken, J., and Styring, S. (1995) *Photosynth. Res. 46*, 177−184.
10. Hoganson, C. W., and Babcock G. T. (1997) *Science 277*, 1953−1956.
11. Force, D. A., Randall. D. W., and Britt, R. D. (1997) *Biochemistry 36*, 12062−12070.
12. Haumann, M., and Junge, W. (1996) in *Oxygenic Photosynthesis: The Light Reactions* (Ort, D. R., and Yocum, C. F., Eds.), pp 165−192, Kluwer Academic Publishers, Dordrecht, The Netherlands.
13. Limburg, J., Szalai, V. A., and Brudvig, G. W. (1999) *J. Chem. Soc., Dalton Trans* 1353−1361.
14. Haumann, M., and Junge, W. (1999) *Biochim. Biophys. Acta 1411*, 86−91.
15. Joliot, P., Barbieri, G., and Chabaud, R. (1969) *Photochem. Photobiol. 10*, 309−329.
16. Kok, B., Forbush, B., and McGloin, M. (1970) *Photochem. Photobiol. 11*, 457−475.
17. Messinger, J., Nugent, J. H. A., and Evans, M. C. W. (1997) *Biochemistry 36*, 11055−11060.
18. Ahrling, K., Peterson, S., and Styring, S. (1997) *Biochemistry 36*, 13148−13152.
19. Messinger, J., Robblee, J., Yu, W. O., Sauer, K., Yachandra, V. K., and Klein, M. P. (1997) *J. Am. Chem. Soc. 119*, 11349−11350.
20. Dexheimer, S. L., and Klein, M. P. (1992) *J. Am. Chem. Soc. 114*, 2821−2826.
21. Yamauchi, T., Mino, H., Matsukawa, T., Kawamori, A., and Ono, T. (1997) *Biochemistry 36*, 7520−7526.
22. Campbell, K. A., Peloquin, J. M., Pham, D. P., Debus, R. J., and Britt, R. D. (1998) *J. Am. Chem. Soc. 120*, 447−448.
23. Campbell, K. A., Gregor, W., Pham, D. P., Peloquin, J. M., Debus, R. J., and Britt, R. D. (1998) *Biochemistry 37*, 5039−5045.
24. Dismukes, G. C., and Siderer, Y. (1981) *Proc. Natl. Acad. Sci. U.S.A. 78*, 274−278.
25. Hansson, O., and Andreasson, L. E. (1982) *Biochim. Biophys. Acta 679*, 261−268.
26. Casey, J. L., and Sauer, K. (1984) *Biochim. Biophys. Acta 767*, 21−28.
27. Zimmermann, J. L., and Rutherford, A. W. (1984) *Biochim. Biophys. Acta 767*, 160−167.
28. Nugent, J. H. A., Turconi, S., and Evans, M. C. W. (1997) *Biochemistry 36*, 7086−7096.
29. Matsukawa, T., Mino, H., Yoneda, D., and Kawamori, A. (1999) *Biochemistry 38*, 4072−4077.
30. Ioannidis, N., and Petrouleas, V. (2000) *Biochemistry 39*, 5246−5254.
31. Zouni, A., Witt, H. T., Kern, J., Fromme, P., Krauss, N., Saenger, W., and Orth, P. (2001) *Nature 409*, 739−743.
32. Boussac, A., Zimmermann, J. L., and Rutherford, A. W. (1989) *Biochemistry 28*, 8984−8989.
33. Sivaraja, M., Tso, J., and Dismukes, G. C. (1989) *Biochemistry 28*, 9459−9464.
34. Ono, T., and Inoue, Y. (1989) *Biochim. Biophys. Acta 973*, 443−449.
35. Hallahan, B. J., Nugent, J. H. A., Warden, J. T., and Evans, M. C. W. (1992) *Biochemistry 31*, 4562−4573.
36. MacLachlan, D. J., and Nugent, J. H. A. (1993) *Biochemistry 32*, 9772−9780.
37. Gilchrist, M. L., Ball, J. A., Randall, D. W., and Britt, R. D. (1995) *Proc. Natl. Acad. Sci. U.S.A. 92*, 9545−9549.
38. Ioannidis, N., and Petrouleas, V. (2002) *Biochemistry 41*, 9580−9588.
39. Ioannidis, N., Nugent, J. H. A., and Petrouleas, V. (2002) *Biochemistry 41*, 9589−9600.
40. Nugent, J. H. A., Muhiuddin, I. P., and Evans, M. C. W. (2002) *Biochemistry 41*, 4117−4126.

41. Guiles, R. D., Yachandra, V. K., McDermott, A. E., Cole, J. L., Dexheimer, S. L., Britt, R. D., Sauer, K., and Klein, M. P. (1990) *Biochemistry 29*, 486-496.
42. Bouges, B. (1971) *Biochim. Biophys. Acta 234*, 102−112.
43. Velthuys, B., and Kok, B. (1978) *Biochim. Biophys. Acta 502*, 211−221.
44. Saygin, Ö., and Witt, H. T. (1985) *Photobiochem. Photobiophys. 10*, 71−78.
45. Beck, W. F., and Brudvig, G. W. (1987) *Biochemistry 26*, 8285−8295.
46. Sivaraja, M., and Dismukes, G. C. (1988) *Biochemistry 27*, 3467−3475.
47. Sivaraja, M., and Dismukes, G. C. (1988) *Biochemistry 27*, 6297−6306.
48. Messinger, J., Wacker, U., and Renger, G. (1991) *Biochemistry 30*, 7852−7862.
49. Messinger, J., and Renger, G, (1993) *Biochemistry 32*, 9379−9386.
50. Riggs-Gelasco, P. J., Mei, R., Yocum, C. F., and Penner-Hahn, J. E. (1996) *J. Am. Chem. Soc. 118*, 2387−2399.
51. Sandusky, P. O., and Yocum, C. F. (1986) *Biochim. Biophys. Acta 849*, 85−93.
52. Beck, W. F., and Brudvig, G. W. (1987) *J. Am. Chem. Soc. 110*, 1517−1523.
53. Ford, R. C., and Evans, M. C. W. (1983) *FEBS Lett. 160*, 159−163.
54. Porra, R. J., Thompson, W. A., and Kriedemann, P. E. (1989) *Biochim. Biophys. Acta 975*, 384−394.
55. Deak, Z., Peterson, S., Geijer, P., Ahrling, K. A., and Styring, S. (1999) *Biochim. Biophys. Acta 1412*, 240−249.
56. Styring, S., and Rutherford, A. W. (1988) *Biochim. Biophys. Acta 933*, 378−387.
57. Krishtalik, L. I. (2000) *Biochim. Biophys. Acta 1458*, 6−27.

BI034116U